

Global Ice and Land Climate Studies Using Scatterometer Image Data

David G. Long

Brigham Young University
459 Clyde Building
Provo UT 84601
long@byu.edu

Mark R. Drinkwater

European Space Agency
ESTEC, Keplerlaan 1, Postbus 299
2200 AG Noordwijk ZH
The Netherlands
Mark.Drinkwater@esa.int

Benjamin Holt and Sasan Saatchi

Jet Propulsion Laboratory
California Institute of Technology
4800 Oak Grove Drive
Pasadena CA 91109
ben@pacific.jpl.nasa.gov
Sasan.Saatchi@jpl.nasa.gov

Cheryl Bertoia

U. S. National Ice Center
4251 Suitland Road
Washington D.C. 20395
bertoiac@natice.noaa.gov

Note: This file is a combined version of two related articles on the Scatterometer Climate Pathfinder. Please use the following references:

Long, D. G., M. R. Drinkwater, B. Holt, S. Saatchi, and C. Bertoia, Global ice and land climate studies using scatterometer image data, EOS Transactions, AGU, 82(43), 503, 2001.

Long, D. G., M. R. Drinkwater, B. Holt, S. Saatchi, and C. Bertoia, Global ice and land climate studies using scatterometer image data, EOS Transactions Electronic Supplement, AGU, http://www.agu.org/eos_elec/010126e.html, 2001.

Global Ice and Land Climate Studies Using Scatterometer Image Data

Spaceborne scatterometers have provided continuous synoptic microwave coverage of the Earth for nearly a decade. Though these scatterometers were originally designed to measure oceanic surface winds, their data are also extremely useful in a broad range of ice and land applications, including the use of extensive scatterometer time series to determine seasonal and interannual variability and possible relationships to climate change. Under a NASA Earth Science Enterprise grant, the Scatterometer Climate Record Pathfinder (SCP) project has produced non-ocean scatterometer imagery and data products that are now publicly available for the first time (<http://www.scp.byu.edu/>).

To date, four spaceborne scatterometers have flown on five different spacecraft (Table 1). NASA launched three scatterometers: the current SeaWinds scatterometer onboard QuikSCAT (QSCAT, 13.4 GHz) launched in 1999; the NASA scatterometer (NSCAT, 14.0 GHz), which flew on the Japanese Space Agency's ADEOS-1 platform during 1996-1997; and the Seasat-A scatterometer system (SASS, 14.6 GHz) which flew in 1978. The European Space Agency's (ESA) 5.3-GHz scatterometer (ESCAT) has been carried onboard both the ERS-1 and ERS-2 satellites since 1991. The SCP project is providing imagery from the three NASA scatterometers in both a unique, enhanced resolution format and an intrinsic resolution format. In addition, new value-added data products from ESCAT are also available.

A scatterometer transmits radar pulses and receives backscattered energy, the intensity of which depends on the roughness and dielectric properties of a particular target. For ice, snow, soil, and vegetation, roughness properties and geometry that affect backscatter include surface roughness, moisture content, leaf size and density, branch orientation, and preferential alignment of surface scatterers. Dielectric properties are affected by physical characteristics of the effective scattering medium or layer—for example, snow grain size, brine concentration in sea ice, and canopy leaf density—as well as by the phase state of water (meltwater on sea ice and land ice, re-frozen percolated melt water in glacial ice, and whether trees are frozen or actively respiring). As scatterometers can be very accurately calibrated to generally to less than a few tenths of a decibel (dB), seasonal and

interannual differences that result in changes in the radar return as low as 1-2 dB may be confidently examined.

The various scatterometer configurations provide additional means for surface discrimination (Table 1). These include the use of different sensor frequencies to isolate surface types, the relative backscatter response between two polarizations (for example, to separate sea ice from open water), the varying backscatter gradient of different surfaces over a range of incidence angles, and the azimuthal response for features with preferred orientations. In general, the sensitivity to surface roughness increases with higher frequencies. The wide swath of scatterometers provides near-daily global coverage, particularly in the polar regions, at intrinsic resolutions generally between 25-50 km, over incidence angles ranging from 20-55°. We note the general trend toward finer resolution with newer sensors.

ESCAT provides the longest scatterometer record. As such, it is invaluable for climate-related investigations. However, due to recent spacecraft attitude and orbital control problems, ESCAT data have been unavailable since January 17, 2001. It is expected that future planned corrections to the ERS-2 spacecraft control will eventually enable continued ESCAT operations later this year. The use of ESCAT in conjunction with the different frequencies of NSCAT and QuikSCAT provides improved discrimination of scattering surfaces, and hence, better understanding. The SASS provides a unique, albeit brief, historical data set that can be compared with the remaining scatterometers to study decadal changes. A recent special issue on scatterometer applications includes 10 papers on ice and land studies, nearly all of which examine seasonal and inter-annual variability and the possible relationship to climate change [*Drinkwater and Lin, 2000*: hereafter referred to as TGARS2000].

Polar Ice

Scatterometer polar imaging applications were first proposed using Seasat SASS followed by ERS wind scatterometer data and have been more recently summarized in

the context of NSCAT [Long and Drinkwater, 1999]. The daily global coverage of the scatterometer in the polar regions and its ability to discriminate sea ice, ice sheets, and icebergs, despite the poor solar illumination and frequent cloud cover of the polar regions, make it an excellent instrument for large-scale systematic observations of polar ice (Figure 1a).

Ice Sheet Applications. Studies of the great ice sheets of Greenland and Antarctica take advantage of the sensitivity of backscatter to the density and size of snow grains in the various ice facies, especially in the percolation zone and during summer melt. This approach provides a means of examining long-term variability over the ice sheets, particularly with ESCAT, including the extent of the seasonal snow melt zone over Greenland and Antarctica (see articles by Wismann on Greenland and Bingham and Drinkwater in TGARS2000). By combining scatterometer data from multiple sensors, the long-term and inter-annual variability of accumulation rates and the extent of seasonal snow melt zones have been estimated over Greenland [Drinkwater *et al.*, 2001] (Figure 2). The greater change in the more recent comparison is corroborated by recent airborne laser profile data that show rapid thinning of the coastal margin of the Greenland ice sheet and also indicate an increased spatial extent of ablation at higher elevations on the western flank of the ice cap. Finally, the azimuthal modulation that is obtained by the suite of scatterometer antennas designed to derive wind direction was found to correlate with directional snow surface features that align with Antarctic katabatic winds (see article by Long and Drinkwater in TGARS2000).

Sea Ice Applications. Over sea ice, the scatterometer is sensitive to roughness and physical properties that vary by ice type and season. Sea ice extent is readily identified with data from ESCAT using a normalized measure of the isotropy of sea ice relative to ocean [Gohin and Cavanié, 1995] and with data from NSCAT and QSCAT (Figure 1b) by comparing the response of vertical transmit-vertical receive (VV) and horizontal transmit-horizontal receive (HH) polarizations over ice and water [e.g., Remund and Long, 1999]. NOAA NESDIS uses polarization differences to separate ice and ocean from QSCAT image products for near real-time products (see

<http://www.natice.noaa.gov/science/products/qs.html>). The National Ice Center (NIC) uses the NESDIS QSCAT ice products in their global ice mapping process, where data from visible, infrared, and passive and active microwave sensors are combined in a manual data assimilation process to produce weekly global sea ice charts [Bertoia *et al.*, 1998]. Initial work with these data show that the QSCAT ice product reliably maps the higher concentrations of the Arctic ice pack, though it less accurately depicts the lighter ice concentrations usually found in the marginal ice zone (Figure 1b). The NIC also expects to attain improved ice forecasting by using QSCAT's accurate depiction of surface winds near the ice edge (Figure 1c). This integrated set of measurements (ice edge and winds) may also be useful for examining turbulent heat fluxes within the marginal ice zones. Arctic field validation of QSCAT sea ice and surface winds was obtained during an October 2001 Barents Sea cruise. Preliminary Antarctic field validation of early operational test data products was performed in 1999-2000.

The onset of seasonal snow melt and freeze-up provides a significant contrast to winter, when conditions over sea ice in the polar regions are colder. Melt onset defines a significant transition in the radiative budget of the ice-covered region, while autumn freeze-up is a key period during which the residual fraction and characteristics of perennial sea ice can be assessed and preconditioning for winter sea ice dynamics is established via the distribution and orientation of newly forming ice in leads. Most recently, algorithmic approaches using scatterometer data to determine melt onset and freeze-up have been examined, including in the Antarctic over a several year period (see article by Drinkwater and Liu in TGARS2000).

Additional studies of sea ice include the derivation of ice velocity fields and ice-type classification. Ice velocity fields are important for estimating heat flux between the ocean and atmosphere, as well as the sea ice mass balance through estimates of ice deformation and growth. Motion fields have been derived using scatterometer data with algorithms based on wavelet analysis [Liu *et al.*, 1999] and cross-correlation with feature tracking [Long and Drinkwater, 1999]. The determination of ice type is another means of estimating mass balance, in addition to being important for navigation. Several recent ice

type studies have been undertaken that often use combined data from one or more scatterometers and other sensors to isolate scattering mechanisms for different ice types, and thereby improve discrimination [e.g., *Kwok et al.*, 1999; see article by Remund et al. in TGARS2000].

Iceberg Tracking. Operationally, the National Ice Center uses QSCAT imagery as a primary source for tracking large icebergs in the Southern Ocean. For example, in 1999, iceberg B-10A—which was 38 km x 77 km in diameter--drifted north out of the pack ice and into the shipping lanes of the Drake Passage (Figure 1). QSCAT was used to track this iceberg from July 1999 until its deterioration in March 2000.

Terrestrial Biosphere Applications

Scatterometer data have also been applied to land studies, making use primarily of changes related to moisture content over both vegetated and bare soil, as well as the seasonal freeze-thaw cycle. Several studies have used the extensive ESCAT time series to examine the derivation of monthly indexes of soil moisture over western Africa (see article by Wagner and Scipal in TGARS2000), seasonal trends in soil moisture content in Spain (see article by Woodhouse and Hoekman in TGARS2000), and the seasonal variability of backscatter over different types of vegetation and land surface covers (see articles by Abdel-Messeh and Quegan, and Frison et al. in TGARS2000). Making use of the change in dielectric constant with phase state (frozen or thawed) of trees, vegetation, and surrounding surface water, as well as the presence or absence of leaves, other studies have used scatterometer data to examine the freeze-thaw cycle of boreal forests [*Kimball et al.*, 2001; see article by Wismann on Siberia in TGARS2000].

In regional- to continental-scale ecological processes, the scatterometer data can provide information about the seasonality of vegetation in terms of availability of moisture and the process of loss or recovery of vegetation. In Africa, within the transition zone between the tropical forest and savanna, the status of the vegetation depends on human activity as well as moisture and rainfall patterns; the scatterometer data capture both the

seasonal and inter-annual variability there (Figure 3). The multitemporal aspect of the data demonstrates that the Northern and Southern Hemisphere ecotone regions have different seasonal dynamics of vegetation and surface moisture. A combination of multi-temporal data from NSCAT and QSCAT at high frequency (14.0 and 13.4 GHz, respectively) and the ESCAT at lower frequency (5.3 GHz) has the potential for identifying the long-term climatic impacts on moisture availability and vegetation loss or recovery.

Available Ice and Land Data Products

The SCP provides two basic forms of gridded image products: 1) a calibrated browse backscatter image at the intrinsic sensor resolution (Table 1); and 2) a unique enhanced resolution image product, which combines multiple overlapping passes over intervals of a few days, or just one using an algorithm called Scatterometer Image Reconstruction (SIR) [Early and Long, 2001]. The resulting enhanced resolutions are about 25 km for ESCAT, 8-10 km for NSCAT and SASS, and either 8-10 km or 5-6 km for QSCAT. In addition, each enhanced image product is decomposed into two sub-images: 1) a backscatter image normalized to the mid-swath incidence angle of 40° (so-called **A** image); and 2) the gradient of backscatter over the range of incidence angles (so-called **B** image). The latter product is not produced for QSCAT because its conically scanning antenna operates at two fixed incidence angles. The enhanced products are well suited for many ice and land studies where the surface backscatter returns are comparatively stable over a 1-2 day period.

These scatterometer image products (as well as ancillary products, documentation, software, movies, and extensive bibliography) are currently available through the SCP data site via file transfer protocol (ftp) (<http://www.scp.byu.edu/>). All processing is done at Brigham Young University's (BYU) Microwave Earth Remote Sensing (MERS) Laboratory. Also, the Jet Propulsion Laboratory's (JPL) Physical Oceanography Distributed Active Archive Center (PODAAC) currently has available browse imagery and raw data for QSCAT (http://podaac.jpl.nasa.gov/quikscat/qscat_data.html). In the

future PODAAC will also be a mirror site for SCP products as well as provide options for obtaining the data on different media. The ESCAT data products are provided by IFREMER-CERSAT to JPL and later transferred to BYU after pre-processing. Future additions to the SCP site include sea ice motion products derived from both NSCAT and QSCAT [Liu *et al.*, 1999] and the capability to select and order large segments of data sets.

We hope that the release of these ice and land scatterometer products through the SCP data site will encourage researchers to use these valuable image data, particularly for climate-related studies. While ESCAT on ERS-2 is presently not collecting data, QSCAT remains fully functional, thus providing a continuation of the recent scatterometer data record that is now nearing a decade. Currently, two known scatterometers are planned for future missions. As a follow-on to QSCAT, NASA's SeaWinds will be flown on NASDA's ADEOS-II mission, which is currently scheduled for launch in early 2002. SeaWinds will essentially have the same configuration as QSCAT and has a mission design lifetime of 5 years. The ESCAT follow-on, ESA's Advanced Scatterometer (ASCAT), will be flown on the first of three METOP satellites and is scheduled for launch in 2005. Each METOP has a design lifetime of 5 years and thus, with overlap, the series has a planned duration of 14 years. ASCAT will be similar to ESCAT in configuration except it will have increased coverage, with two 500-km swaths (one on each side of the spacecraft nadir track). Thus, with scatterometers likely to continue for many years, the applications of scatterometer data for long time-scale ice and land applications will also continue and likely thrive.

Acknowledgments

The Scatterometer Climate Record Pathfinder task is supported by NASA's Office of Earth Science Enterprise through Research Announcement 99-OES-04. ESCAT data were provided by CERSAT-IFREMER as part of ESA Project AO2.USA.119. MRD completed this work at the Jet Propulsion Laboratory and subsequently at the European Space Agency. The JPL effort was supported by NASA through a contract with JPL,

California Institute of Technology. The use of QuikScat data at the National Ice Center was facilitated by Paul Chang at NOAA's Office of Research and Applications and by the excellent work of scientific programmer Mike Chase. Figure 1C is provided courtesy of Son Nghiem, Jet Propulsion Laboratory.

References

Bertoia, C., J. Falkingham, and F. Fetterer, Polar SAR data for operational sea ice mapping, in *Recent Advances in the Analysis of SAR Data of the Polar Oceans*, edited by R. Kwok and C. Tsatsoulis, Springer Verlag, Berlin, 201-234, 1998.

Drinkwater, M. R., and C. C. Lin, Introduction to the special section on emerging scatterometer applications, *IEEE Trans. Geosci. Remote Sens.*, 38, 1763-1764, 2000.

Drinkwater, M. R., D. G. Long, and A. W. Bingham, Greenland snow accumulation estimates from scatterometer data, *J. Geophys. Res.*, PARC Special Issue, in press, 2001.

Early, D. S., and D. G. Long, Image reconstruction and enhanced resolution imaging from irregular samples, *IEEE Trans. Geosci. Remote Sens.*, 39, 291-302, 2001.

Gohin, F., and A. Cavanié, A first try at identification of sea ice using the three beam scatterometer of ERS-1, *Int. J. Remote Sens.*, 16, 2031-2054, 1995.

Kimball, J. S., K. C. McDonald, A. C. Keyser, S. Frohling, and S. W. Running, Application of the NASA scatterometer (NSCAT) for determining the daily frozen and nonfrozen landscape of Alaska, *Remote Sens. Environ.*, 75, 113-126, 2001.

Kwok, R., G. F. Cunningham, and S. Yueh, Area balance of the Arctic Ocean perennial ice zone: October 1996 to April 1997, *J. Geophys. Res.*, 104, 25747-25759, 1999.

Liu, A., Y. Zhao, and S. Y. Wu, Arctic sea ice drift from wavelet analysis of NSCAT and SSM/I data, *J. Geophys. Res.*, 104, 11529-11538, 1999.

Long, D. G., and M. R. Drinkwater, Cryosphere applications of NSCAT data, *IEEE Trans. Geosci. Remote Sens.*, 37, 1671-1684, 1999.

Remund, Q., and D. G. Long, Sea-ice extent mapping using Ku-band scatterometer data, *J. Geophys. Res.*, 104, 11,515-11,527, 1999.

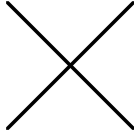
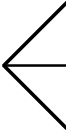
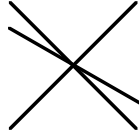
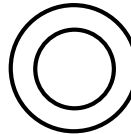
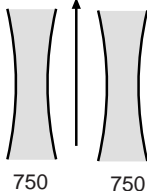
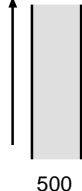
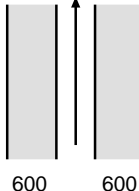
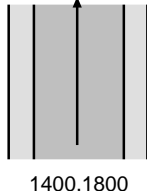
	SASS	ESCAT	NSCAT	SeaWinds
FREQUENCY	14.6 GHz	5.3 GHz	14.0 GHz	13.4 GHz
ANTENNA AZIMUTH ORIENTATIONS				
POLARIZATIONS	V-H, V-H	V ONLY	V, V-H, V	V-OUTER/H-INNER
BEAM RESOLUTION	FIXED DOPPLER	RANGE GATE	VARIABLE DOPPLER	PENCIL-BEAM
MODES	MANY	SAR, WIND	WIND ONLY	WIND/HI-RES
RESOLUTION	50/100 km	25/50 km	25/50 km	25 km/6x25 km
SWATH, km	 750 750	 500	 600 600	 1400,1800
INCIDENCE ANGLES	0° - 70°	18° - 59°	17° - 60°	46° & 54°
DAILY COVERAGE	VARIABLE	< 41 %	78 %	92 %
DATES	SEASAT 6/78—10/78	ERS-1 1992—96 ERS-2 1995—	ADEOS I 8/96—6/97	QuikSCAT 6/99— ADEOS II ~02/02

Table 1. Characteristics of four spaceborne scatterometers flown on Seasat (SASS), ERS-1/2 (ESCAT), ADEOS (NSCAT), and QuikSCAT (SeaWinds or QSCAT).

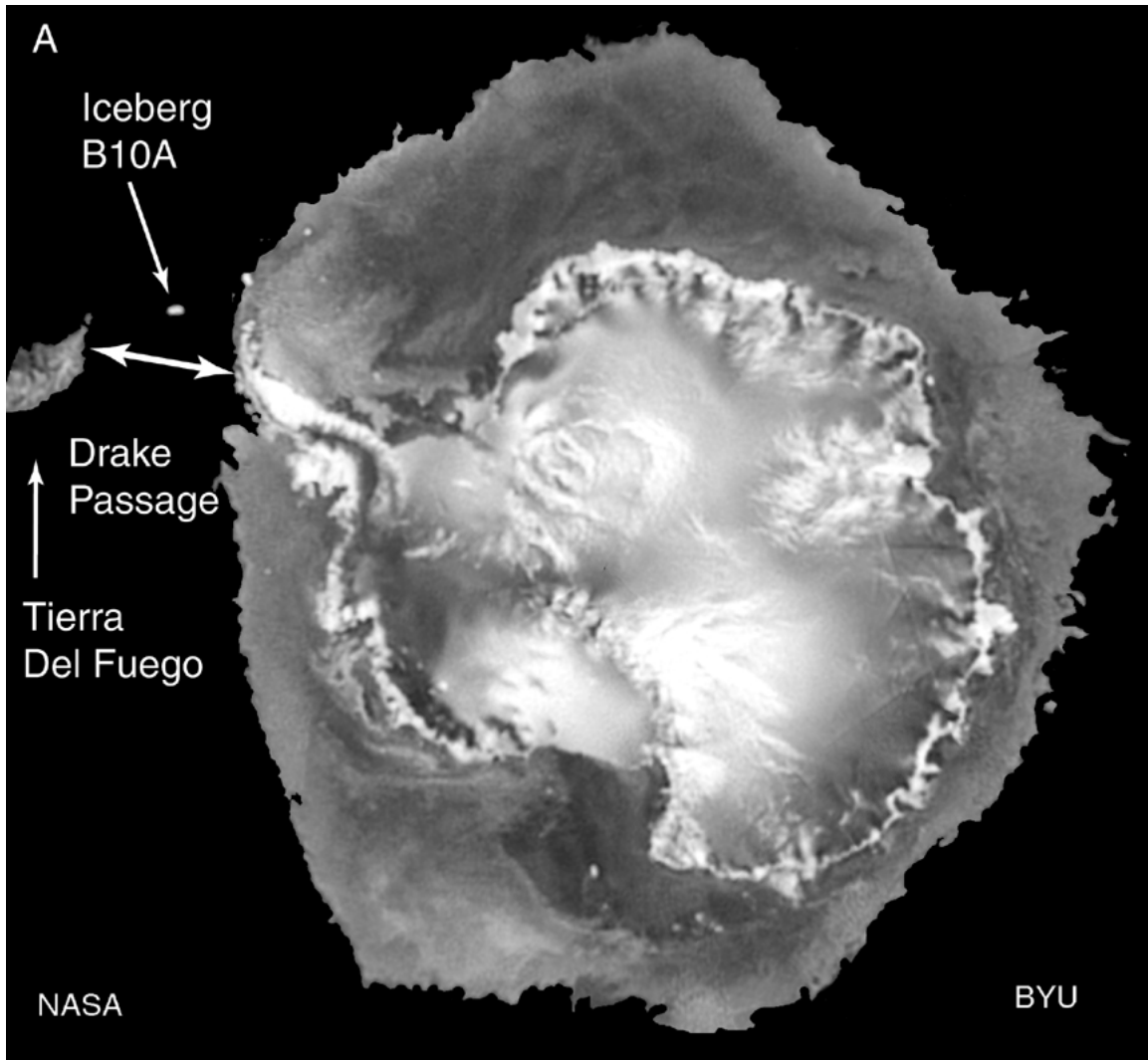


Figure 1A. This QSCAT image shows Antarctica and surrounding sea ice cover in July 1999. Iceberg B10A (50 km x 100 km) is identified in Drake Passage and eventually melted near South Georgia Island in March 2000. Iceberg B10 broke off Thwaites Glacier in 1992 and split into two in June 1995. The complicated backscatter over the continent is related to ice and snow characteristics, surface and subsurface topography, katabatic winds, and melt zones. The variations in sea-ice returns are due to the snow cover, thickness, and history of the ice since formation.

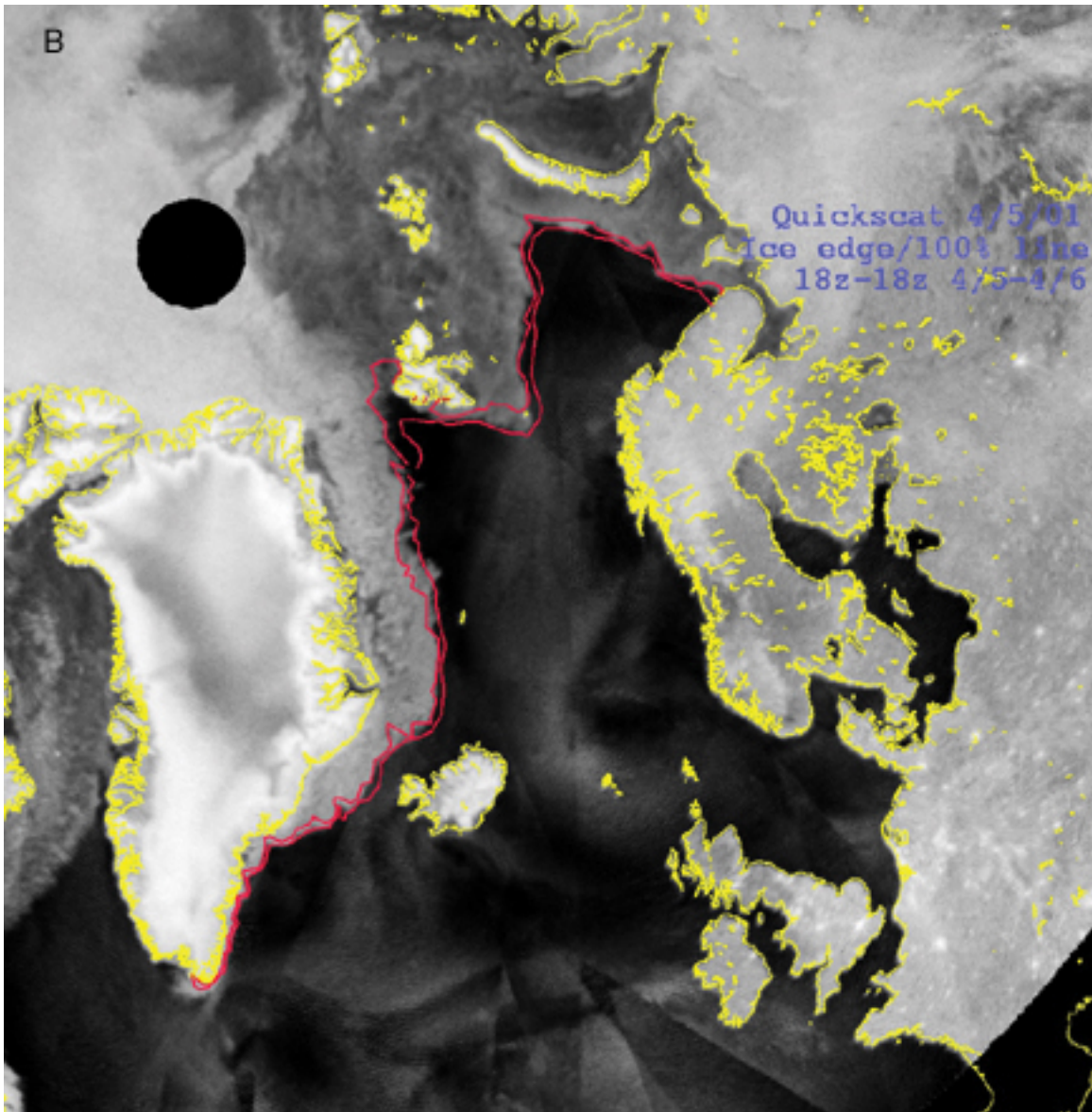


Figure 1B. The QSCAT ice product of the Barents and East Greenland Seas is shown for April 5, 2001. Overlaid in red is the 100% ice concentration line derived from QSCAT and the southern limit of all known ice line, produced through analysis of visible, infrared, and SAR data by the NIC.

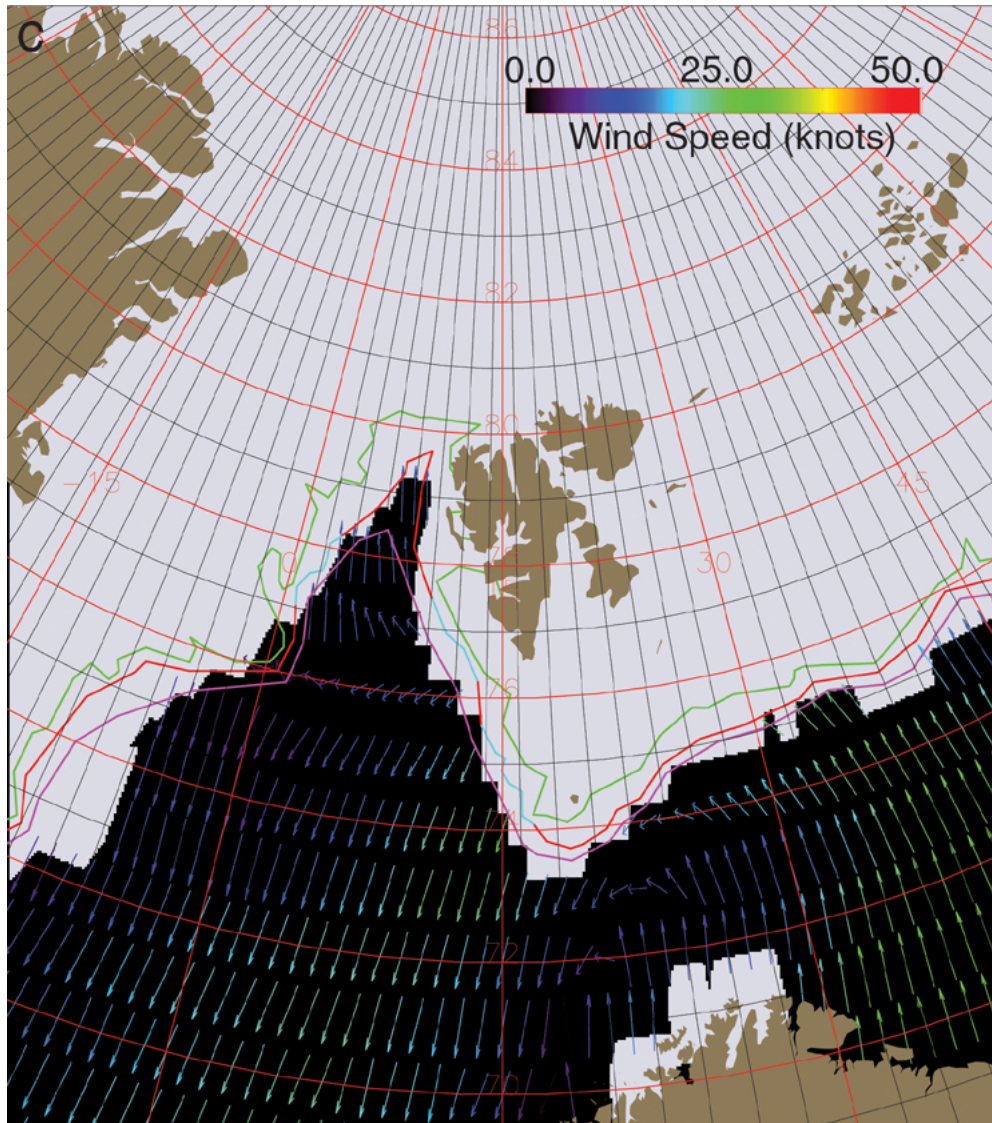


Figure 1C. A prototype product shows the NIC's analyzed ice edge (green is 100 % ice concentration), QSCAT-derived ice edge (light blue), and ocean surface wind vectors from April 5, 2001. The wind vectors are used to forecast expected ice edge movement over a 24-hour period (cyan).

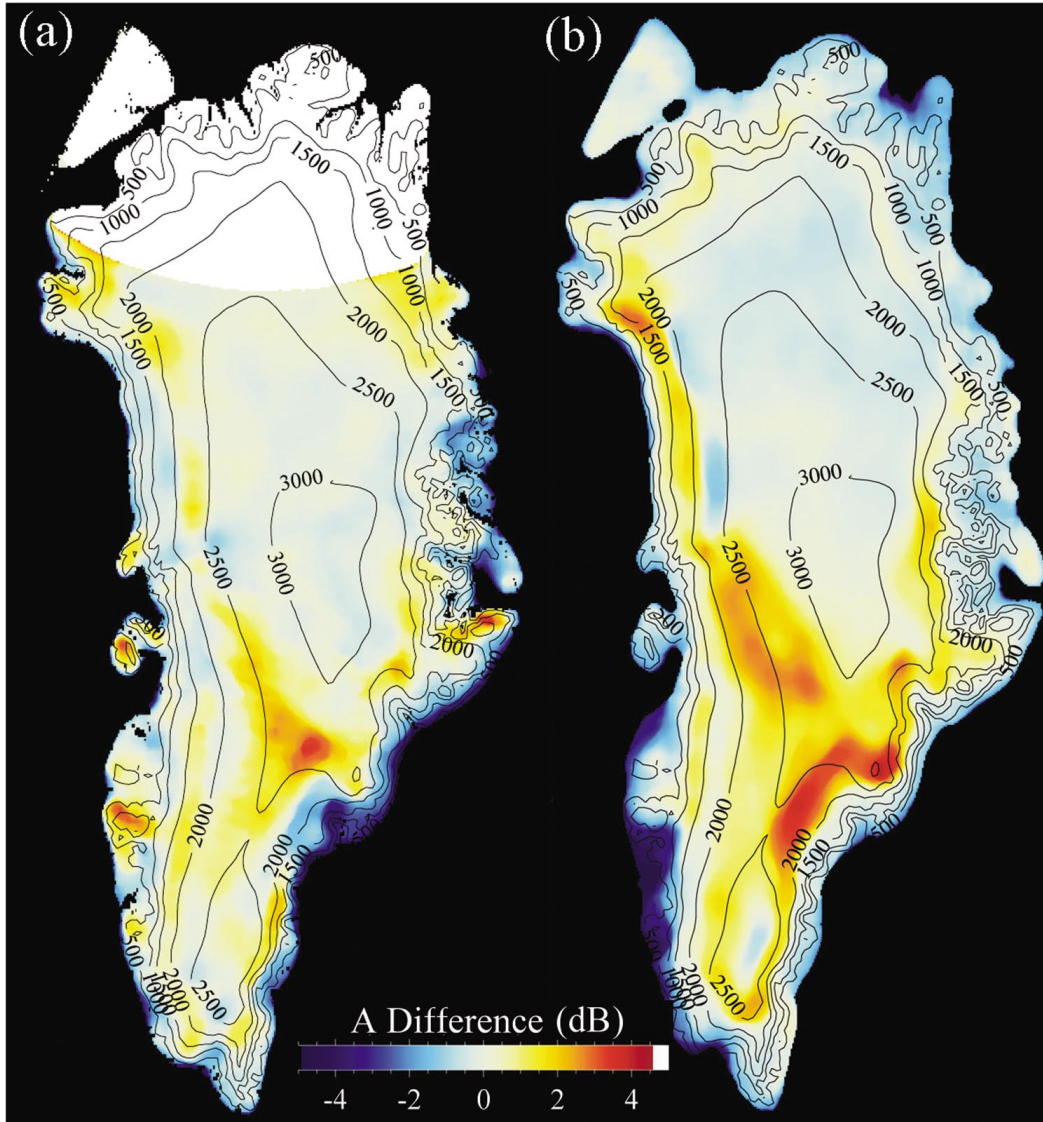


Figure 2. Scatterometer data from SASS, NSCAT, and QSCAT over Greenland are used to monitor changes in melt extent and snow accumulation in response to inter-annual and decadal climate variability. Positive differences in vertical polarization images normalized to a 40 degree incidence angle indicate increases in scattering by buried ice lenses formed during summer melt. The differences between a) SASS and NSCAT (1978 and 1996) are significantly less than those between b) NSCAT and QSCAT (1997 and 2000).

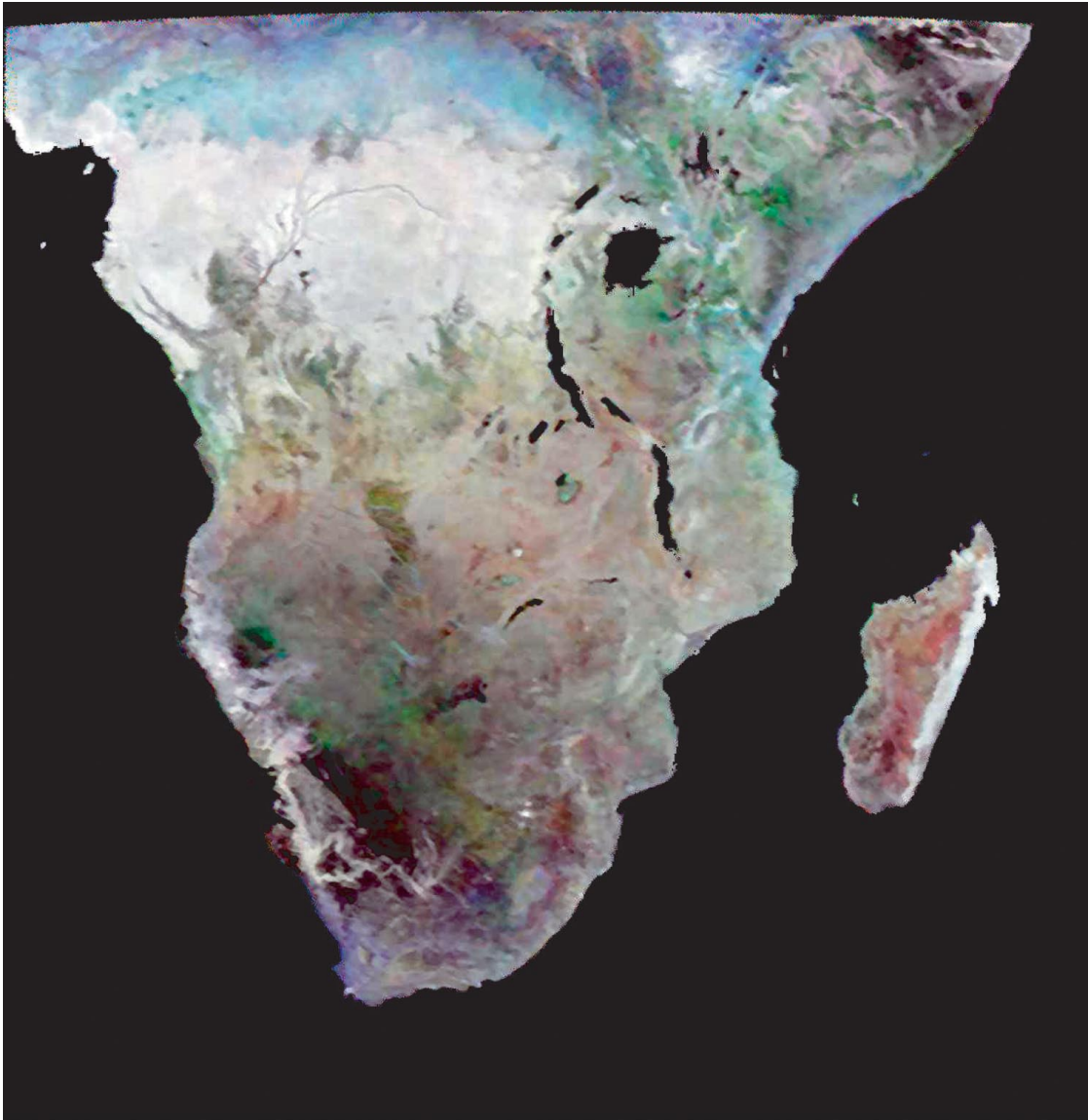


Figure 3. In this NSCAT vertical polarization multi-temporal image of central and south Africa, the colors represent three dates of NSCAT composite images from October 1996 (red), March 1997 (green), and June 1997 (blue). The color image clearly separates the band of woodland savanna and ecotone regions in the northern and southern boundaries of the evergreen tropical forest (saturated in white). Backscatter variations are due to surface moisture and seasonality of vegetation.